F. J. RICH, R. A. HEELIS, W. B. HANSON, P. B. ANDERSON, B. J. HOLT,
L. L. HARMON, D. R. ZUCCARO, C. R. LIPPINCOTT, D. GIROUARD, and W. P. SULLIVAN

COLD PLASMA MEASUREMENTS ON HILAT

A major objective of the HILAT mission is to study the disturbance of radio signals passing through the turbulent, ionized gas or plasma of the ionosphere. Because the disturbance is proportional to the density of the plasma through which the signal is passing, most of the disturbance occurs at altitudes of 300 to 500 km, several hundred kilometers below the satellite. Cold plasma (less than 1 electronvolt, corresponding to 13,000 K) measurements are made at the location of the spacecraft in order to determine the large-scale variations of density with respect to the latitude and the flow speed of the plasma. These parameters are known to affect plasma turbulence at altitudes of 300 to 500 km and are only slightly affected by the difference in altitude from there to the spacecraft. Plasma turbulence at the spacecraft altitude is also being measured, but the relationship between local turbulence and turbulence below the spacecraft has not yet been established.

INSTRUMENTS

The cold plasma measurements on the HILAT satellite are made by an ion drift meter, an ion retarding potential analyzer, and a spherical, electron Langmuir probe. In Fig. 1, the three sensors are shown attached to their mounting bracket and the ground plane. Figure 2 shows the position of the thermal sensors on the leading edge of the spacecraft.

The ion drift meter with its square aperture measures the flux of thermal ions onto the spacecraft y-z plane (x is directed forward) and the angle of arrival of the thermal ions. From the angle of arrival and knowledge of the spacecraft attitude and velocity, the cross-track components of the flow of the ionized atmosphere (or ionospheric plasma) can be determined. The ion-retarding potential analyzer with its circular aperture measures the flux of thermal ions onto the spacecraft y-z plane and their energy spectrum. The total ion flux is used to determine the total density of the local ionospheric plasma. From an analysis of the ion energies, we can determine the major ion species and concentrations, the electrostatic potential of the spacecraft, and the ram component of the plasma flow. The electron sensor (Langmuir probe) was intended to measure the omnidirectional flux of cold electrons. However, a malfunction resulted in the measurement of only the omnidirectional flux of suprathermal electrons (energies greater than approximately 1 electronvolt). The ground plane around the ion sen-

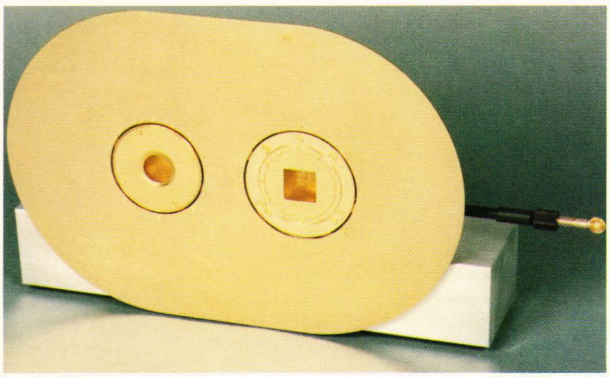

Figure 1 — View of the sensors and ground plane for the Thermal Plasma Experiment as they would look when mounted on the spacecraft.

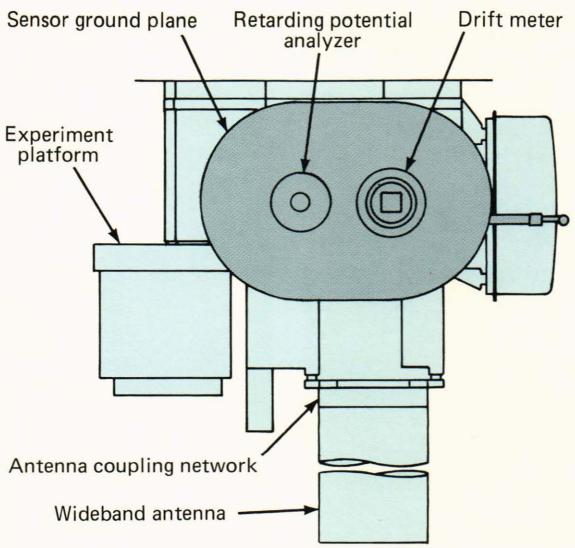

Figure 2 — Frontal view of the arrangement of experiments on the lower or earthward portion of the spacecraft. The sensors and ground plane of the Thermal Plasma Experiment are attached to the top of the experiment deck. The electronics box is attached to the bottom of the experiment deck. They are connected by a cable that runs along the edge of the experiment deck.

sors is used to provide a uniform electrostatic surface around the planar apertures. It is maintained slightly below the ambient plasma potential by an active feedback device.[1]

A detailed description of the sensors is given in Ref. 2. They are very similar to ones that have been flown on the Atmospheric Explorer[3] and Dynamics Explorer[4,5] satellites and used in the Defense Meteorological Satellite Program.[6,7]

Satellite operations are divided into telemetry frames of 0.5 second of spacecraft time. (1.000 second in spacecraft time equals 0.99956 second in real time. All time spans given here are in spacecraft time.) The electronics for the Thermal Plasma Experiment starts its frame with the start of the read-out gate that lags the start of frame pulse by 375 milliseconds. The experiment frame is divided into 64 equal time slots by a 128 hertz counter. The telemetry words are sampled according to the time slot in which they occur. The data are sampled and stored 5.13 milliseconds after the beginning of the time slot.

EARLY ORBIT MEASUREMENTS

The performance of the sensors can be shown with data that were obtained in July 1983 for an early orbit checkout of the satellite. In particular, we will show data obtained on July 23, 1983 (Day 204), at approximately 2000 universal time (UT), from a tracking station near Kiruna, Sweden. The digital data at that time were on the 400 megahertz channel. The time was chosen because this was a high-latitude pass similar to anticipated operational passes and because a minor geomagnetic storm with significant substorms was in progress. The data are noisy because of a geophysical disturbance of the ionosphere and because of scintillation of the telemetry reception at 400 megahertz, which is not present in L-band telemetry.

Based on the precipitating electron and Auroral Image Mapper data for this pass over Kiruna (see Fig. 4 in the paper in this issue by Fremouw and Wittwer and also the cover of this issue), the geophysical environment that the satellite passed through can be described. When the satellite's telemetry was acquired, it was in the region of the evening diffuse aurora. The diffuse aurora appears in optical sensors, including the Auroral Ionospheric Mapper, as a subvisual, nearly uniform glow 2 to 6° wide in latitude and extending around the auroral oval. The diffuse aurora is on the equatorward side of the bright, discrete aurora. Between approximately 69,570 and 69,660 seconds UT, the satellite was on field lines connected to the bright, discrete auroral features. Between 69,690 and 69,990 seconds UT, the satellite was crossing the polar cap, where a weak flux of low-energy particles, known as the polar rain, was precipitating. From 69,990 seconds UT to the end of the pass, the satellite was in a very disturbed morning auroral zone.

Figure 3 shows the ion density, which is measured by the ion drift meter with a resolution of one point every 2 seconds, and 1 second averages of the horizontal and vertical components of the ion drift with re-

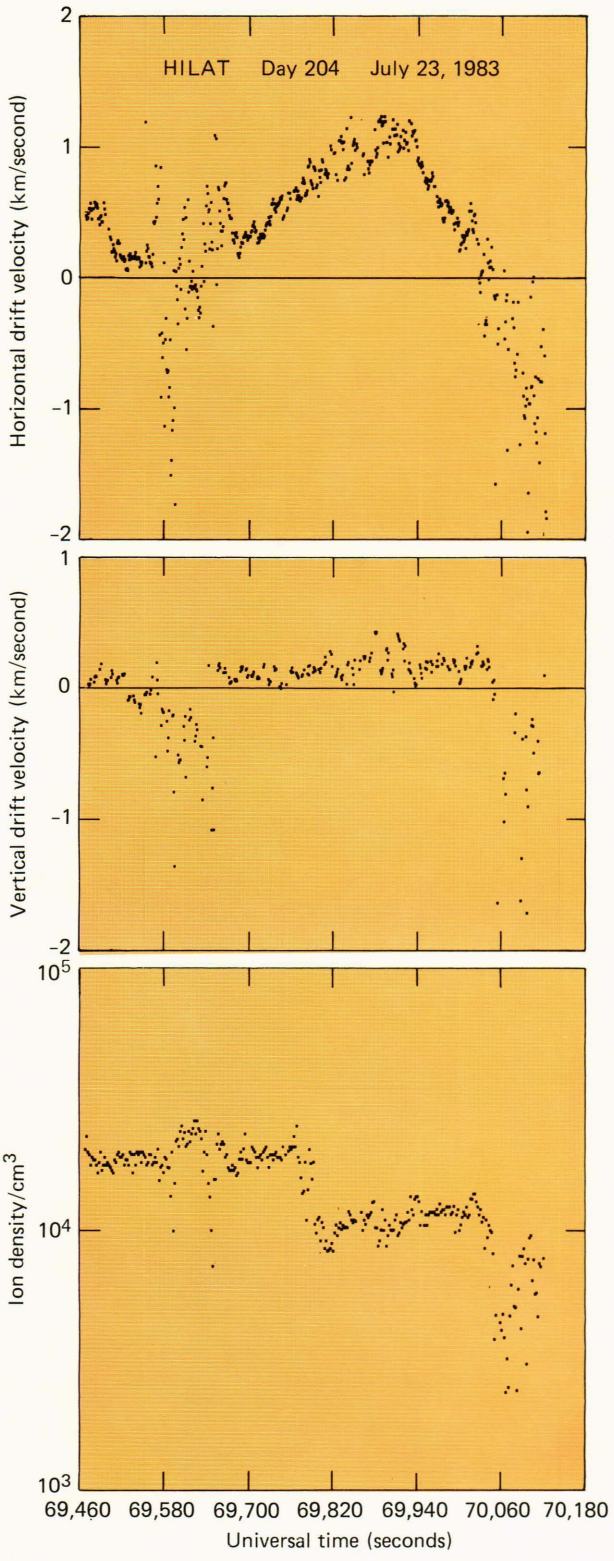

Figure 3 — Data from the ion drift meter obtained during a passage acquired on July 23, 1983, by the tracking station near Kiruna, Sweden. The telemetry starts when the satellite was in the evening (1800 magnetic local time) diffuse aurora region. The satellite proceeded into the evening discrete aurora region, across the polar cap, and into the morning (0100 magnetic local time) discrete aurora region, where the telemetry was lost.

spect to spacecraft coordinates. There is a gradient in the density from the beginning to the end of the pass that is related to the increasing solar zenith angle. There is also evidence for enhanced density (lower panel) in the region of the evening diffuse aurora and a definite enhancement in the density near 69,600 seconds UT that is related to the discrete aurora. Although many local density enhancements are related to the precipitating particle flux, there is no one-to-one correlation.

An obvious feature of the ion drift is the slow (25 to 50 minute) variation in the horizontal component caused by the spacecraft oscillations. The variations with scale sizes of 5 minutes and less are variations in the local plasma caused by the discrete auroras and other high-latitude effects. The nominal spacecraft oscillations were estimated to be $\pm 2°$ after the initial oscillations were damped out. This corresponds to a slow variation of ± 0.25 km/second in the drift meter data. Since the observed variation in the drift data is greater than expected, we assume that the spacecraft oscillations are greater than predicted.

Figure 4 shows data from the horizontal component of the drift meter, the y axis of the magnetometer, and the zenith detector of the particle spectrometer during the passage of the spacecraft through the region of the evening discrete auroras. The magnetometer data are shown with two samples per second and with the background geomagnetic field removed. Positive deflections are westward, and negative deflections are eastward. Positive slopes represent Birkeland currents out of the ionosphere (which implies a net flux of electrons into the ionosphere), and negative slopes represent Birkeland currents into the ionosphere (a net flux of electrons out of the ionosphere). The electron flux represents the integral of flux into all the channels of the zenith detector. In the diffuse aurora region, the average energy of the precipitating electrons is a few kiloelectronvolts. In the region of the discrete aurora, the average energy is approximately 200 to 300 electronvolts.

The drift meter data in Fig. 4 show the full resolution available for the horizontal drift, which alternates every 4 seconds between 16 and 32 samples per second. The first few seconds of data are typical of moderately quiet conditions in the ionosphere. There is an instrument noise level of 30 to 40 meters/second peak-to-peak. The average drift speed is offset from zero by approximately the corotation velocity of the plasma plus some amount because the x axis is misaligned from the velocity vector. The misalignment in the horizontal plane (yaw) seems to yield a slowly varying value between 0 and 500 meters/second.

Near 69,561 seconds, there is an oscillation in the horizontal component with a peak-to-peak amplitude of 700 meters/second. This corresponds exactly with a small region of precipitating, low energy (20 to 600 electronvolt) electrons. We have observed this kind of oscillation in a number of passes of early orbit data. Because this structure and others similar to it have a sinusoidal shape, it is postulated that this represents plasma turbulence with a scale size of approximately 1 km. Of the cases observed so far, we have noticed that these structures are always associated with soft precipitation, but there are regions where the precipitation is nearly identical in energy but there is no signature in the drift meter data. Preliminary analysis indicates that the flux intensity is also important to

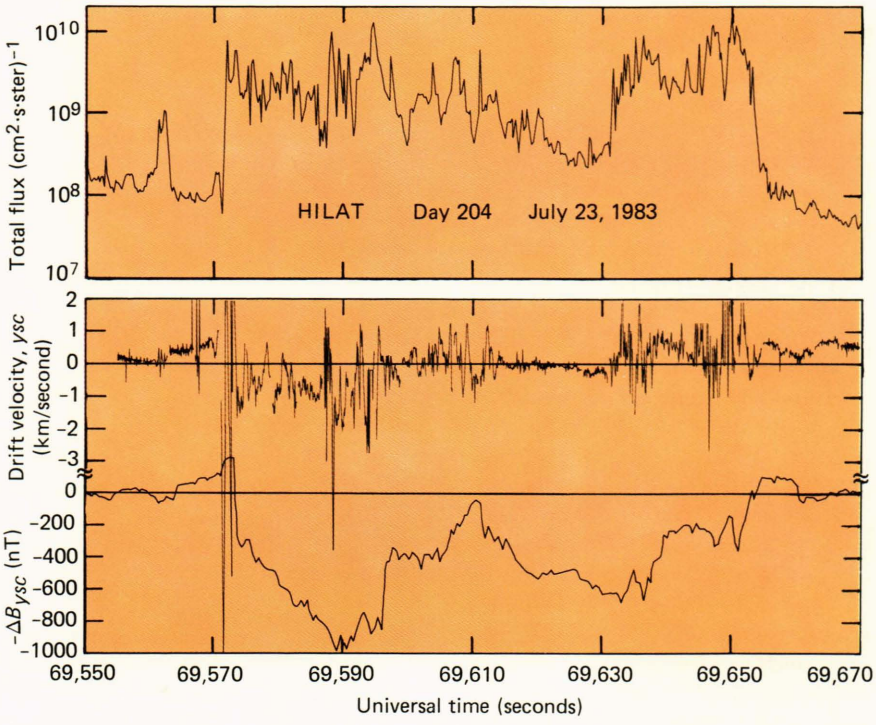

Figure 4 — The horizontal component of the drift is presented at full temporal resolution together with two samples per second of the magnetometer data and four samples per second of the integrated flux of electrons into the zenith detector of the particle spectrometer. These data are from the section of the passage shown in Fig. 3 when the spacecraft was in the region of the discrete aurora. The spacecraft +y axis was directed eastward. The horizontal drift and the magnetometer east-west component are presented so that the deflections for an evening auroral zone are typically negative.

the appearance of small-scale, sinusoidal variations in the horizontal drift.

The smooth oscillations in the horizontal drift at 69,561 seconds UT are overshadowed by very strong, irregular oscillation in the horizontal drift as the spacecraft entered the region of the discrete auroras. The excursions of the horizontal drift between 69,570 and 69,572 seconds UT go to the maximum limits of the detector. Since each excursion represents several points, there is little doubt that the data are representative of the activity in the environment. However, the magnitude of the drift speeds greater than 3.5 km/second is not reliable since the instrument is designed to respond to drifts in a linear manner for magnitudes less than 3.5 km/second. At 69,572 seconds, there is an extremely large change in the magnetic field deflection of approximately 450 nanoteslas in one-half second or roughly 94 microamperes per square meter into the ionosphere. (Usually any field-aligned current larger than 2 microamperes per square meter is considered to be large.) Since the strongest plasma turbulence is observed near this extraordinary field-aligned current, it is tempting to suggest that the turbulence is a function of it.

The oscillations in the horizontal drift are observed throughout the discrete aurora region with varying magnitudes and scale lengths, as shown in Fig. 4. There is some correlation between the steepness of the slope of the magnetic deflections (or the field-aligned current) and the degree of disturbance of the plasma drift velocity, but the correlation is not one-to-one. There is also a correlation between the flux of the soft precipitating electrons and the disturbance in the plasma drift, but again the correlation is not one-to-one. For example, in the region of 69,620 to 69,639 seconds UT, the plasma drift disturbance is suppressed, and both the field-aligned current and precipitating electrons are weaker than in adjacent regions. Thus, both the field-aligned current and the flux of soft electron precipitation are probably related to the plasma drift disturbance. However, the precipitating soft electrons seem to be the dominant factor. If this is true, then the sinusoidal variation near 69,561 seconds and the chaotic variations in the discrete aurora region are related. The chaotic disturbance may be the nonlinear case of the sinusoidal disturbance.

In order to show the influence of soft electrons, data from a passage through the region of the dayside cusp are shown in Figs. 5 and 6, which are in the same format as Figs. 3 and 4. The data were obtained from Sondre Stromfjord, Greenland, at L band by the first operational receiver. Again, the spacecraft oscillation is very prominent in the horizontal drift velocity data in Fig. 5. In Fig. 6, the region of very soft electron precipitation (average energy less than 100 electronvolts) associated with the dayside cusp is shown with the full-resolution horizontal drift data. Again, the horizontal drift shows a small-scale disturbance associated with the intense, soft precipitation.

We could show many passes through the auroral zone with precipitation of kiloelectronvolt electrons

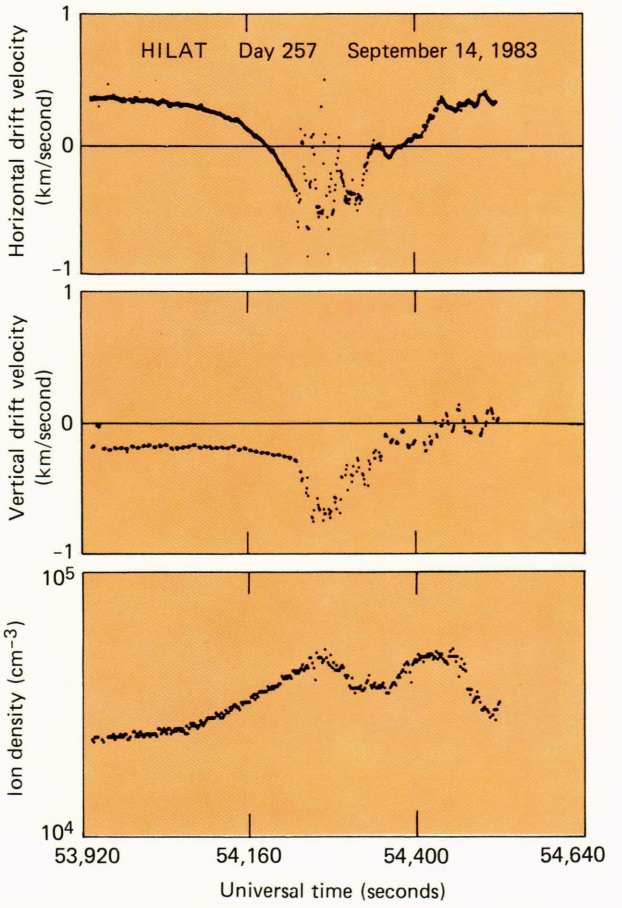

Figure 5 — Data from the ion drift meter in a format similar to Fig. 3. The telemetry was acquired on September 14, 1983, on L band from Sondre Stromfjord, Greenland. The data start when the satellite was near 65° magnetic latitude and 1130 magnetic local time. The middle section of the data was acquired when the satellite was in the region of the dayside cusp. Telemetry was lost as the satellite proceeded into the dayside polar cap.

and field-aligned currents but with no small-scale disturbance in the horizontal drift. Thus we conclude that precipitation of soft electrons is the dominant factor in the creation of these small-scale horizontal drift disturbances.

One of the principal uses of the electron Langmuir probe sensor in the Thermal Plasma Experiment was to monitor the local plasma density and oscillations in that density. The DC current from the electron sensor as shown in Fig. 7 is not fulfilling this function. For a thermal plasma with a density between 10^4 and 10^5 electrons/cm^3, the telemetry output for the DC current should be between 3 and 4 volts. Although it is not reading the expected value, the sensor is clearly responding to something. An analysis of these data and of the construction of the experiment have led us to believe that the connection from the electronics to the outer grid is broken, but that the lead to the inner collector is intact. The outer grid is floating at an electrostatic potential specified by the random currents from the environment to the sensor, which is approx-

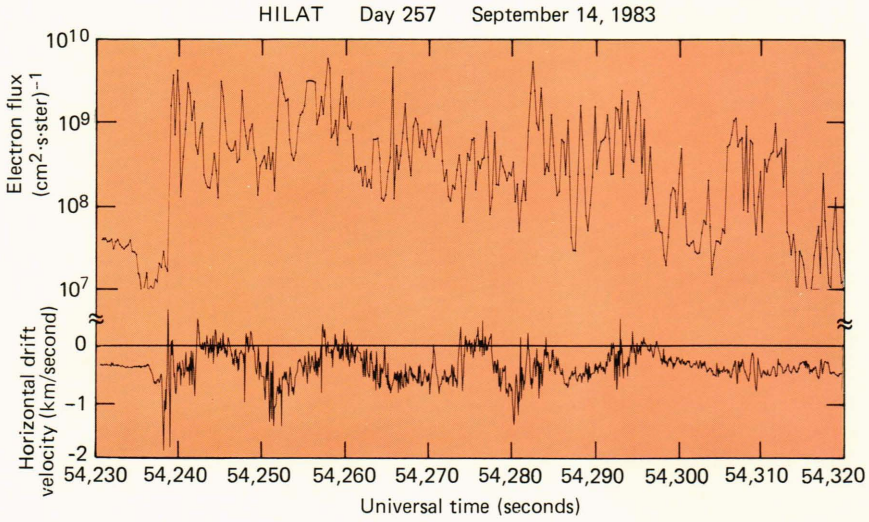

Figure 6 — The horizontal component of the drift is presented at full temporal resolution together with the integrated flux of electrons into the zenith detector of the particle spectrometer. These data are the section of the pass shown in Fig. 5 when the satellite was in the region of the dayside cusp. The average energy of the precipitating electrons is approximately 100 electronvolts in this region.

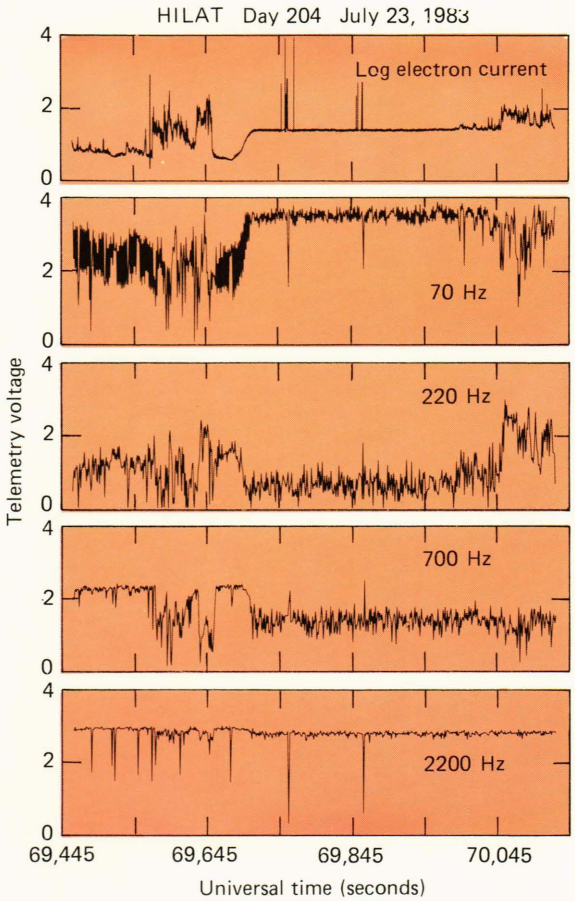

Figure 7 — The DC and AC components of the current to the spherical electron sensor for the time period of Fig. 3 are presented in telemetry units. For the electron current, each unit of telemetry voltage is a power of 10 increase in the collected current. For the four filters, each unit of telemetry voltage represents a change of − 10 decibels in the root-mean-square of the collected electron current at 70, 220, 700, or 2200 hertz.

imately − 1 volt. Thus 99.9% of the thermal electrons are deflected away from the outer grid. Any electron outer grid. Any electron with an energy greater than the grid and is measured. Thus we have an omnidirectional, suprathermal electron probe. The peaks in the measurements between 69,530 and 69,670 seconds UT represent current from the precipitating electron flux.

The four filter channels connected to the electron sensor that were intended to measure small-scale oscillations in the ionospheric plasma are obviously working, although they are not measuring what was expected. The filter channels were set to read 2.5 to 3.0 volts when the environment was quiet and to decrease by 1 volt per 10 decibels of increasing oscillation strength. The first three filters are responding to oscillations in the precipitating electron flux. The cutoff in the fluctuations suggests that the precipitating electrons are modulated by something like the ion cyclotron frequency.

The retarding potential analyzer determines the energy of ions impacting on the plane of the aperture. This is done by stepping the potential on a screen between the aperture and the collection plate. The current collected decreases as the potential barrier exceeds the energy of part or all of the incoming ion population. If the spacecraft velocity, attitude, and potential are known, then the retarding potential analyzer data can be used to determine the component of the bulk ion drift normal to the aperture plane. In addition, the temperature and the atomic species of the ions can be determined. There are two requirements that must be met in order to turn the data into all of the above geophysical parameters. First, there must be several data points near the potential associated with the average energy of each ion species. Second, the geophysical environment cannot change significantly during the time it takes to collect one sequence of current versus voltage.

Several sets of raw data are shown in Fig. 8. The times are part of the time span shown in Figs. 3 and 4. Since the spacecraft attitude is not known, the spacecraft velocity vector has been assumed to be parallel to the aperture normal. The potential of the sensor ground with respect to the plasma is not known but

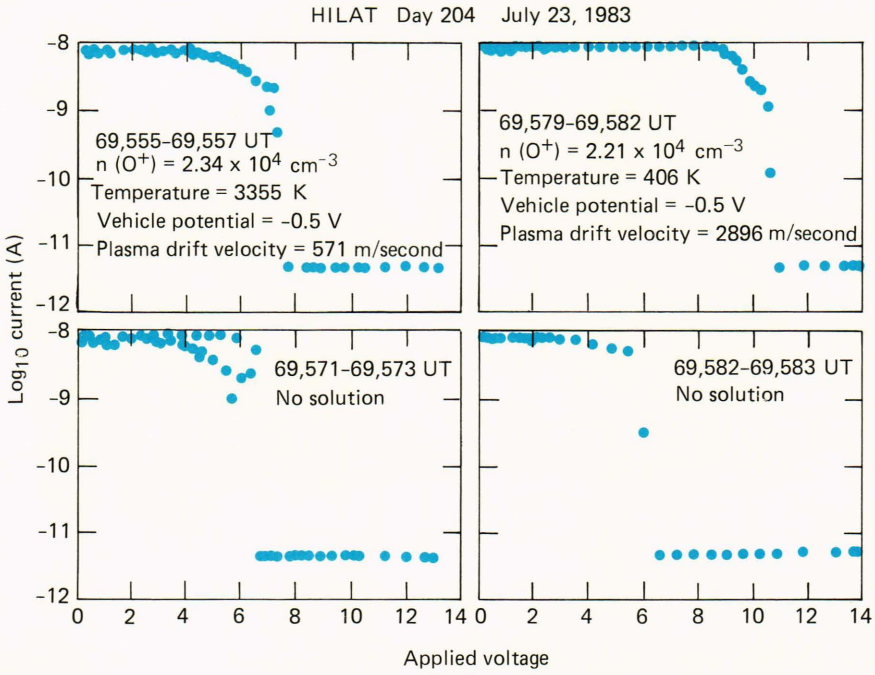

Figure 8 — The current-versus-voltage curves for the ion retarding potential analyzer for a few time intervals during the Kiruna passage shown in Fig. 3. The sequences on the left are three 0.667 second sequences that have been combined for analysis as one 2 second sequence. The sequences on the right are a 3 second and a 1 second sequence. Positive values of drift are in the ram (−x) direction.

is assumed to be −0.5 volt. These two assumptions lead to an inaccuracy of a few hundred meters per second in the calculated drift velocities. The calculated values for the 3 second period beginning at 69,555 seconds UT are quite reasonable. Actually, this current-versus-voltage sequence is not one sequence, but three sequences that have been combined to facilitate the data processing. Because the analysis of the data is a curve-fitting procedure, it can consume large amounts of computer time. Since the geophysical environment was stable for the 2 second span, the algorithm was able to find an answer. The data for the 2 second span beginning at 69,571 seconds UT show that the environment was definitely not stable, and no solution was found by the algorithm. In fact, the three individual sequences can clearly be seen in the plot of current versus voltage. If the three sequences were processed separately, solutions might be found. The 3 second span beginning at 69,579 seconds UT is a single sequence that occurs once every 32 seconds in the instrument's cycle. At this time, the geophysical environment was disturbed but not enough to prevent the algorithm from finding a solution. For the 1 second span beginning at 69,582 seconds UT, there are not enough data points near the critical voltage (6 volts in this case) to define the current-versus-voltage curve for the curve-fitting algorithm.

As shown by Fig. 8, the retarding potential analyzer data can complement the two drift components obtained from the drift meter. However, the processing of the data is not as straightforward. This will result in many occasions when a generalized fitting algorithm will fail to find a solution in a disturbed geophysical environment. However, with some human intervention, an adequate solution can be found in some, although not all, cases.

REFERENCES

[1]D. R. Zuccaro and B. J. Holt, "A Technique for Establishing a Reference Potential on Satellites in Planetary Atmospheres," *J. Geophys. Res.* **87**, 8327-8329 (1983).

[2]F. J. Rich and R. A. Heelis, *Preliminary Data Processing Plan for the Thermal Plasma Experiment on the HILAT Satellite,* Air Force Geophysics Lab. TR-83-0091 (1983).

[3]W. B. Hanson, D. R. Zuccaro, C. R. Lippincott, and S. Sanatani, "The Retarding Potential Analyzer on Atmospheric Explorer," *Radio Sci.* **8**, 5483-5501 (1973).

[4]W. B. Hanson, R. A. Heelis, R. A. Power, C. R. Lippincott, D. R. Zuccaro, B. J. Holt, L. H. Harmon, and S. Sanatani, "The Retarding Potential Analyzer for Dynamics Explorer B," *Space Sci. Instrum.* **5**, 1503-1510 (1981).

[5]R. A. Heelis, W. B. Hanson, C. R. Lippincott, D. R. Zuccaro, L. H. Harmon, B. J. Holt, J. E. Doherty, and R. A. Power, "The Ion Drift Meter for Dynamics Explorer B," *Space Sci. Instrum.* **5**, 511-521 (1981).

[6]M. Smiddy, R. C. Sagalyn, W. P. Sullivan, P. J. L. Wildman, P. Anderson, and F. J. Rich, *The Topside Ionosphere Plasma Monitor (SSIE) for the Block 5D/Flight 2 DMSP Satellite,* Air Force Geophysics Lab. TR-78-0071 (1978).

[7]F. J. Rich, M. Smiddy, R. C. Sagalyn, W. J. Burke, P. Anderson, S. Bredesen, and W. P. Sullivan, *In-Flight Characteristics of the Topside Ionospheric Monitor (SSIE) on the DMSP Satellite Flight 2 and Flight 4,* Air Force Geophysics Lab. TR-80-0152 (1980).